CLM - R 194

UKAEA

Report

A SMALL IGNITION TOKAMAK WITH NEUTRAL BEAM ADDITIONAL HEATING

J J FIELD
E MINARDI
E SALPIETRO

CULHAM LABORATORY
Abingdon Oxfordshire

1979

C/18

Available from H. M. Stationery Office

£1

CLM - R 194

CLM-R 194

A SMALL IGNITION TOKAMAK WITH NEUTRAL BEAM ADDITIONAL HEATING

by

J.J. FIELD, E. MINARDI and E. SALPIETRO*

Culham Laboratory, Abingdon, Oxon, OX14 3DB, UK

(Euratom/UKAEA Fusion Association)

ABSTRACT

The two most successful tokamaks currently in operation are PLT and Alcator, the former achieving the highest temperatures and the latter the highest value of $n\tau_E$. We present transport calculations for a small ignition tokamak (SIT) which we envisage to operate with intense neutral injection heating, like PLT, and with a high field, high current density and high particle density, like Alcator. Besides the physics of such a device we also include some technological considerations, based mainly on the design of the Frascati tokamak.

*CNEN-EURATOM Association - JET

November 1978

SBN 85311 077 8

1. INTRODUCTION

Small high density tokamaks have proved to be very successful in their operation, for example regarding their high $n\tau_E$ values and low impurity content [1, 2]. Hence it is a natural consequence [3] to consider a machine to follow on from the Alcator and Frascati tokamaks, with the aim of achieving thermonuclear ignition. However, it appears that such a device would be unlikely to reach the required conditions using only ohmic heating [4] and a strong dependence on alpha particle heating for reaching ignition [5]. Further, such a device, without significant additional heating would not constitute a route towards a tokamak reactor.

Since it is clear that additional (to ohmic) heating will be necessary for a tokamak reactor and neutral injection heating has proved to be very successful in current experiments [18], an obvious course is to consider a high field experiment with neutral injection heating, to demonstrate ignition.

In this paper we present some calculations for a small tokamak whose main parameters are given in the appendix. On the basis of not particularly optimistic assumptions, i.e. ion thermal transport worse than neo-classical [18], the numerical results indicate that thermonuclear ignition might be achieved in a device whose principal technological requirements have been successfully demonstrated already.

The outline of this paper, which is the sequel to [4], is as follows. Section 2 gives the eight basic differential equations which are solved and describes the general approach, section 3 contains an account of the neutral beam heating and section 4 the treatment of thermonuclear reactions and alpha particle heating. Section 5 describes the various source functions assumed for the plasma transport equations, while section 6 discusses some preliminary technological considerations. Sections 7 and 8 contain the numerical results and discussion, and conclusions, respectively. Mks units are used throughout, with the exception of energies which are in keV, unless otherwise stated.

2. TRANSPORT EQUATIONS

The radial dependence is averaged out of the equations by assuming density and temperature profiles of the form,

$$n(r) = n_o(1 - r^2/a^2)^{\delta/2} \quad , \tag{2.1}$$

$$T(r) = T_o(1 - r^2/a^2)^{\delta} . \tag{2.2}$$

If $\delta > 0$, as we assume to be the case, this averaging introduces certain weighting factors into the differential equations [4], however to simplify the present discussion we take $\delta = 0$.

Since high density Tokamaks operate with $Z_{eff} = 1$ [1] we confine our attention to deuterium, tritium, electrons and alpha particles, with particle densities n_D, n_T, n_e and n_α respectively. In this connection we note that the behaviour of Alcator appears to be modelled reasonably well with the neglect of impurity transport [6], however impurity radiation losses are implicitly included to some extent in our assumptions about electron energy transport - see section 5. We assume that the plasma ions, with the exception of the fast alpha particles and fast beam-injected deuterons, are all at the same background temperature T_i with a density n_x.

The transport equations solved are for the electron and ion energy densities, the fuel and alpha particle densities, tritium ratio, ε, [4], the energy density of the fast alphas created by thermal D-T reactions, E_α, the energy density of the beam deuterons, E_B, and the energy density of the beam-induced fast alphas, $E_{B\alpha}$. So the equations take the form

$$\frac{d}{dt}\left(\frac{3}{2} n_e K T_e\right) = \sum_\ell S_\ell^e \tag{2.3}$$

$$\frac{d}{dt}\left(\frac{3}{2} n_x K T_i\right) = \sum_\ell S_\ell^i \tag{2.4}$$

$$\frac{dn_F}{dt} = \sum_\ell R_\ell^F \tag{2.5}$$

$$\frac{dn_\alpha}{dt} = \sum_\ell R_\ell^\alpha \tag{2.6}$$

$$\frac{d\varepsilon}{dt} = \varepsilon(1 - \varepsilon)(2\varepsilon - 1)n_F\overline{\sigma v} + (\varepsilon_R - \varepsilon)R_F/n_F + R_B^\varepsilon + R_{B\alpha}^\varepsilon \tag{2.7}$$

$$\frac{dE_\alpha}{dt} = -\frac{E_\alpha}{\tau_\alpha} + \frac{S_\alpha}{P_\alpha} \tag{2.8}$$

$$\frac{dE_B}{dt} = -\frac{E_B}{\tau_B} + S_B \tag{2.9}$$

$$\frac{dE_{B\alpha}}{dt} = -\frac{E_{B\alpha}}{\tau_{B\alpha}} + S_{B\alpha} , \tag{2.10}$$

where $K = 1{\cdot}6 \times 10^{-16}$ joule/keV in (2.3) and (2.4). In (2.7) n_F is the fuel particle density, $n_F = n_D + n_T$, $\overline{\sigma v}$ is the fusion cross-section for the DT reaction averaged over a Maxwellian distribution, ϵ_R is the tritium ratio of the refuelling gas, R_F is the refuelling coefficient and R_B^ϵ and $R_{B\alpha}^\epsilon$ are defined in section 3. In (2.8) - (2.10) the τ's represent slowing-down times, while P_α is the alpha-particle non-escape probability; the fact that P_α enters (2.8) is a consequence of our definition of S_α, the thermal fusion energy density delivered to the plasma per unit time.

The electron particle density, n_e, is calculated on the assumption of quasi-neutrality.

3. NEUTRAL BEAM HEATING

In describing the neutral beam heating, which we take to be a deuteron beam, several aspects have to be considered:

1. The beam penetration, trapping, and coupling efficiency,
2. The slowing down of the beam and the division of its energy between the electrons and ions,
3. Fusion reactions induced by the fast beam deuterons colliding with the thermal tritons,
4. The effects of the beam on the particle density and the tritium ratio.

One of the main difficulties with neutral injection heating is the problem of beam penetration and it is well known that this is particularly acute for plasmas in the thermonuclear regime. Suppose that the energy confinement time $\tau_E \sim \bar{n}a^2$[7], then

$$\bar{n}\tau_E = \text{const. } \bar{n}^2 a^2 \qquad (3.1)$$

where $\bar{n}$ is the mean density. For injection of deuterium into a cylindrical plasma the beam penetration, assuming $1/e^2$ attenuation, is given by [8]

$$C_{pen} = \bar{n}a\ 10^{-17}/(5{\cdot}5\ W_B) \qquad (3.2)$$

where a is the minor radius of the device and W_B is the beam injection energy in keV. Hence we see that with the widely accepted scaling (3.1) the Lawson product $\bar{n}\tau_E$ is limited by the beam injection energy. In particular, taking the energy confinement time to be given by [7],

$$\tau_{Ee} = 3{\cdot}2 \times 10^{-21} q_a^{\frac{1}{2}} a^2 \bar{n}_e , \qquad (3.3)$$

with $q_a = 2.5$ and $C_{pen} = 1$, with $W_B = 160$ keV we find $\bar{n}_e \simeq 2{\cdot}3 \times 10^{20} m^{-3}$ and $n_e \tau_E \simeq 0{\cdot}4 \times 10^{20} m^{-3} s$. This limitation on the Lawson product would mean that ignition could never be achieved; fortunately this difficulty can be circumvented as described in section 7, by suitably programmed gas puffing.

The trapping of the fast deuteron can be estimated on the basis of its gyroradius and the width of its banana orbit. The resulting non-escape probability for radial injection is given by [33],

$$P_B = \exp\left[- \frac{4\left(\frac{1}{2} + q_a\right)\left(KW_B m_D/3\right)^{\frac{1}{2}}}{e\, B_T\, a}\right] , \qquad (3.4)$$

where m_D is the deuteron mass and e is the magnitude of the electronic charge. The beam coupling efficiency is given in terms of the beam penetration

$$C_{eff} = C_{pen} \exp\,(1 - C_{pen}) . \qquad (3.5)$$

The slowing down time of the fast beam deuterons, τ_B, and the fractions of beam energy that go to the electrons and ions, f_{Be} and f_{Bi} $(= 1 - f_{Be})$ respectively, are calculated on the basis of the classical theory of the slowing down of fast particles in a plasma [8, 9]. For deuterons the slowing down time is given by

$$\tau_B = \frac{1{\cdot}32 \times 10^{19} T_e^{3/2}}{n_e \ln \Lambda_e} \ln\left\{1 + \frac{6{\cdot}08 \times 10^{-3} n_e (2 + \varepsilon)}{\left(n_F + n_\alpha (2 + \varepsilon)\right)} \left(\frac{W_B}{T_e}\right)^{3/2}\right\} \qquad (3.6)$$

and

$$f_{Be} = 2x\left[\frac{1}{2x} - \frac{1}{6}\,\ell n\left\{\frac{1 - x^{-\frac{1}{2}} + x^{-1}}{(1 + x^{-\frac{1}{2}})^2}\right\} - \frac{1}{\sqrt{3}}\tan^{-1}[(2x^{-\frac{1}{2}} - 1)/\sqrt{3}] - \frac{1}{\sqrt{3}}\tan^{-1}\left(\frac{1}{\sqrt{3}}\right)\right] \tag{3.7}$$

where

$$x = \frac{30 \cdot 2}{(2 + \varepsilon)^{\frac{2}{3}}}\,\frac{T_e}{W_B} \,. \tag{3.8}$$

Having calculated the beam slowing down time τ_B we now have to consider the source term for the energy density of the beam deuterons, S_B, in (2.9). We define the beam "current" by

$$I_B = P_{N.I.}/(W_B K) \text{ particles } s^{-1} \,, \tag{3.9}$$

where $P_{N.I.}$ is the power rating of the neutral injectors, then

$$S_B = W_B I_B K C_{eff}/V \equiv K E_{BIN} \,, \tag{3.10}$$

where V is the plasma volume

$$V = 2\pi^2 R_o a^2 \tag{3.11}$$

The source terms in the transport equations due to the beam generated alpha particles will be considered in sections 4 and 5, but here we will consider the effect of the beam on the particle density balance. The source term in (2.5) due to the beam deuterons is

$$R_B^F = E_{BIN} P_B/W_B \tag{3.12}$$

while in the equation for the tritium ratio (2.7) we have

$$R_B^\varepsilon = E_{BIN} P_B \varepsilon/(W_B n_F) \,. \tag{3.13}$$

4. THERMONUCLEAR REACTIONS AND ALPHA PARTICLE EFFECTS

We confine our attention to the D-T reaction since the cross-section for the D-D reaction is very small in comparison [10] for $T_i \simeq 10$ keV.

Although the main source of thermonuclear reactions is due to the thermal DT plasma, for which we take the following fit of BRUNELLI [11] for the cross-section averaged over a Maxwellian distribution,

$$\overline{\sigma v} = 9 \times 10^{-22} \exp\left[- 0{\cdot}476 \left| \ell n\left(\frac{T_i}{69}\right)\right|^{2{\cdot}25} \right] , \quad T < 69 \text{ keV} , \quad (4.1)$$

there are also a significant number of fusion reactions due to the high energy beam reacting with the thermal tritons. For these reactions we take the following fit to the cross-section [10],

$$\sigma(W) = [W\{\exp(A1/\sqrt{W}) - 1\}]^{-1} [A2/\{1 + (A3W - A4)^2\} + A5] \quad (4.2)$$

where W is the energy of the incident deuteron in eV and the constants A1 to A5 are

$$A1 = 1453 \sqrt{eV} , \quad A2 = 502 \times 10^5 \text{ eV barn} , \quad A3 = 1368 \times 10^{-8}/\text{eV}$$

$$A4 = 1{\cdot}076 , \quad A5 = 409 \times 10^3 \text{ eV barn}$$

The problems arising from the thermonuclear reactions and the presence of alpha particles are formally the same as those of the neutral beam heating discussed in section 3. The alpha particle non-escape probability, P_α, slowing down time τ_α and the thermal fusion energy density delivered to the plasma per unit time, S_α, have all been given previously [4]. In calculating power densities, etc. $\overline{\sigma v}$ is evaluated at the peak ion temperature $T_{i,o}$ and the resulting differential equations typically involve a weighting factor, C_4, given by

$$C_4 = \int_0^1 (1 - y)^\delta \exp\left\{ - 0{\cdot}476 \left| \ell n\left[\frac{T_{i,o}(1 - y)^\delta}{69}\right]\right|^{2{\cdot}25} + 0{\cdot}476 \left| \ell n\left(\frac{T_{i,o}}{69}\right)\right|^{2.25} \right\} dy . \quad (4.3)$$

The other weighting factors entering the equations through the profile averaging have been given previously [4], as have the fractions of alpha energy that go to the electrons and ions, $f_{\alpha e}$ and $f_{\alpha i}$ $(= 1 - f_{\alpha e})$, respectively.

In equation (2.10) for the energy density of the beam-induced alpha particles we take $\tau_{B\alpha} = \tau_B + \tau_\alpha$ and the source of the power density, $S_{B\alpha}$,

$$S_{B\alpha} = \frac{E_{BIN}\, W_\alpha\, n_F\, P_B\, \varepsilon K}{W_B} \int_0^{\tau_D} \sigma v(t)\,dt \qquad (4.4)$$

where W_α = 3520 keV, v(t) is calculated from the energy of the slowing-down deuteron,

$$W(t) = \frac{1}{2} m_D v^2 = W_B \left\{ (\gamma + 1) e^{-t/\tau_D} - \gamma \right\}^{2/3} \qquad (4.5)$$

with

$$\gamma = \frac{16{\cdot}4\ [n_F + n_\alpha(2 + \varepsilon)]}{n_e(2 + \varepsilon)} \left(\frac{T_e}{W_B}\right)^{3/2} \qquad (4.6)$$

$$\tau_D = \frac{1{\cdot}32 \times 10^{19}\, T_e^{3/2}}{n_e\, \ell n\, \Lambda_e} \qquad (4.7)$$

and σ is given by (4.2).

The thermonuclear reactions affect the particle balance in the system due to the depletion of fuel ions and the production of alpha particles. The loss of fuel due to the fusion reactions of the thermal deuterons and tritons is given by

$$R_\alpha^F = -\ 2\, n_F^2 \varepsilon (1 - \varepsilon) \overline{\sigma v}\ . \qquad (4.8)$$

The loss of beam deuterons as a result of beam-plasma fusion reactions is represented by

$$R_{B\alpha}^F = -\ \frac{P_B\, n_F\, E_{BIN}\, \varepsilon}{W_B} \int_0^{\tau_D} \sigma v(t)\,dt \qquad (4.9)$$

The source of alpha particles due to thermal fusion reactions is given by

$$R_{th}^\alpha = -\ \frac{1}{2}\, R_\alpha^F\, P_\alpha\ , \qquad (4.10)$$

while the source of alphas due to beam-plasma fusions is

$$R_B^\alpha = -\ R_{B\alpha}^F\, P_\alpha\ . \qquad (4.11)$$

The change in the tritium ratio due to the loss of tritons as a consequence of beam-plasma fusions is accounted for by the term

$$R_{B\alpha}^\varepsilon = -\ \frac{I_B\, C_{eff}\, n_T (1 - \varepsilon) P_B}{V\, n_F} \int_0^{\tau_D} \sigma v(t)\,dt\ . \qquad (4.12)$$

5. SOURCE FUNCTIONS APPEARING IN THE TRANSPORT EQUATIONS

The source functions appearing in the electron energy equation (2.3) are the following

S^e_Ω , ohmic heating

S^e_B , electron heating by neutral beam

S^e_α , electron heating by alpha particles produced by thermal fusions

$S^e_{B\alpha}$, electron heating by alpha particles produced by beam-plasma fusions

S^e_Δ , electron-ion collisional transfer

S^e_{br} , bremsstrahlung radiation

S^e_{cy} , cyclotron radiation

S^e_{tr} , electron transport losses by conduction and convection

S^e_R , electron energy source arising from cold gas refuelling

The following electron energy sources have been given previously [4]: S^e_Ω , S^e_α , S^e_Δ , S^e_{br} , S^e_{cy} [12, 13], S^e_{tr} , and will not be repeated here. However, in this context, we note that since S^e_{tr} involves the electron energy confinement time τ_{Ee} ,

$$S^e_{tr} = - 1{\cdot}5\ n_e K T_e/\tau_{Ee} , \qquad (5.1)$$

where τ_{Ee} is given by the empirical Alcator scaling (3.3), we are implicitly including some power loss through impurity line radiation. Terry et al. [2] state that impurity line radiation accounts for $\sim$10% of the total ohmic input power at high densities in the Alcator tokamak.

The source term for electron heating by the neutral beam is

$$S^e_B = f_{Be}\ E_B\left[P_B + \tfrac{1}{2}\ (1 - P_B)\right]\Big/\tau_B , \qquad (5.2)$$

and for the electron heating by alpha particles generated by beam-plasma fusions

$$S^e_{B\alpha} = f_{\alpha e}\ E_{B\alpha}\left[P_\alpha P_B + \tfrac{1}{2}\ (1 - P_\alpha P_B)\right]\Big/\tau_{B\alpha} . \qquad (5.3)$$

where $\tau_{B\alpha} = \tau_B + \tau_\alpha$. The cold gas refuelling gives rise to the source term

$$S^e_R = R^F_R\ K\ W^e_F , \qquad (5.4)$$

where R^F_R is the source rate for fuel particles, i.e. gaspuffing, W^e_F is the

energy of the cold electrons.

The source terms on the right hand side of the ion energy equation (2.4) are,

S^i_Δ , ion-electron collisional transfer (= $- S^e_\Delta$)

S^i_{tr} , ion transport losses by conduction and convection

S^i_α , ion heating by alpha particles produced by thermal fusions

$S^i_{B\alpha}$, ion heating by alpha particles produced by beam-plasma fusions

S^i_B , ion heating by the neutral beam

S^i_R , ion energy source arising from cold gas refuelling .

The ion energy transport losses,

$$S^i_{tr} = - 1{\cdot}5\ n_x K T_i / \tau_{Ei} . \qquad (5.5)$$

are more pessimistic than neoclassical for our example since we take [4, 14],

$$\tau_{Ei} = (T_e/T_i)\tau_{Ee} . \qquad (5.6)$$

The source term for ion heating by alpha particles generated by beam-plasma fusions is

$$S^i_{B\alpha} = f_{\alpha i}\ E_{B\alpha}\left[P_\alpha P_B + \tfrac{1}{2}\ (1 - P_\alpha P_B)\right]/\tau_{B\alpha} . \qquad (5.7)$$

The ion heating by the neutral beam gives rise to the source

$$S^i_B = f_{Bi}\ E_B \left[P_B + \tfrac{1}{2}\ (1 - P_B)\right] / \tau_B . \qquad (5.8)$$

Refuelling with cold gas gives the source term

$$S^i_R = R^F_R\ K\ W^i_F , \qquad (5.9)$$

where W^i_F is the energy of the cold ions. The expression for S^i_α has been given previously [4].

The following source terms for fuel particles appear in (2.5),

R^F_D , diffusive loss of fuel particles

R^F_R , source of cold neutral gas with tritium ratio ε_R

R^F_B , source of deuterons due to neutral beam

$R^F_{B\alpha}$, loss of fuel (tritium) due to beam-plasma fusions,

R_{α}^{F} , loss of fuel due to thermal fusion reactions

$R_{B\alpha}^{F}$, loss of beam deuterons due to beam-plasma fusions

From the results of the Alcator tokamak it appears that the particle confinement time, τ_p , scales in the same way as the energy confinement time, at least up to $\bar{n}_e = 10^{20} m^{-3}$, and that $\tau_p \simeq 4 \tau_E$. Hence for the diffusive loss of fuel particles we take,

$$R_D^F = - n_F / \tau_p \qquad (5.10)$$

with

$$\frac{1}{\tau_p} = (1 - R_c)/\tau_{Ei} \qquad (5.11)$$

with the recycling coefficient $R_c = 0{\cdot}75$. The assumed behaviour, as a function of time, of the source of cold neutral gas is described in sections 6 and 7. R_B^F is given by (3.12), $R_{B\alpha}^F$ by (4.9) and R_{α}^F by (4.8).

The equation for the time evolution of the alpha particle density, (2.6), contains the following source functions

R_B^{α} , source of alpha particles due to beam-plasma fusion reactions

R_{th}^{α} , source of alpha particles due to thermal fusion reactions

R_D^{α} , sink of alpha particles due to diffusive losses,

where R_B^{α} is given by (4.11), R_{th}^{α} by (4.10) and [4],

$$R_D^{\alpha} = - n_{\alpha} / \tau_p \qquad (5.12)$$

6. TECHNOLOGICAL ASPECTS

6.1 General remarks

The philosophy of the SIT design is based mainly on the experience gained during the construction and commissioning of the Frascati tokamak [19], however it has to match the new requirements such as neutral injection heating, and the absence of a copper shell.

6.2 Toroidal magnet [20]

The toroidal magnet is to consist of twelve modules, the radial forces acting on each module are supported from outside. Between two modules there is a gap of $3^{\circ}30'$ to allow access for neutral injection, plasma diagnostics, vacuum pumping and the assembly of the vacuum

chamber. After assembly the gap will be filled with a wedge to ensure mechanical continuity on the outer radius of the magnet. The low current density in the toroidal magnet coils at the outer major radius can be increased near both sides of a port, in order to reduce the toroidal magnetic field ripple. The maximum current density is $J = 113$ A/mm^2 and the maximum stress, calculated as for FT, is $\sigma = 25{\cdot}3$ kg/mm^2 ; these numbers compare favourably with the current density and mechanical stress in FT : $J_{FT} = 166$ A/mm^2, $\sigma_{FT} = 26{\cdot}2$ kg/mm^2, and allow us to have a plateau of about 2 s and to feel confident in its performance. The ohmic power dissipated at - 200°C is 22·5 MW.

An estimation of the ohmic power dissipated at the end of the plateau is ~ 100 MW, then the total energy needed is ~ 500 MJ. This energy is composed of 220 MJ of magnetic energy and 280 MJ of ohmically dissipated energy. The low magnetic energy stored in the toroidal magnet allows a short current rise time and with a reasonable power supply system one could expect a rise time of 2 s. To have a short rise time it is necessary to apply a voltage per turn higher than the voltage needed at the end of the plateau. For example, if we choose 240 turns for the magnet the current per turn is 208 kA, the voltage per turn 2 V and the voltage applied to the magnet is 480 V. Hence, for the magnet a voltage ten times higher in the rising phase than in the plateau phase, can easily be applied.

6.3 Poloidal field system

The poloidal field system must supply the magnetic flux and the equilibrium field. The plasma magnetic flux for the peaked plasma current distribution is

$$\phi_p = L_p I_p = 4{\cdot}20 \ \text{Wb}, \qquad (6.1)$$

if $L_p = 1{\cdot}147$ μH and $I_p = 2{\cdot}85$ MA. This magnetic flux can be supplied by a transformer similar to the FT transformer [21] ($\phi = 4{\cdot}20$ Wb for one swing and an external radius of $R_T = 0{\cdot}35$ m). We will have a reserve of flux for the losses during the start up phase and during the current plateau in the plasma because our transformer radius is 0·4 m instead of 0·35 m. We can use a double swing, and in addition, part of the vertical field for the plasma equilibrium produces flux linked with the plasma.

6.4 The vacuum vessel and neutral injection

Two technical solutions can be envisaged for the vacuum chamber:

(a) Continuous toroidal bellows of 2 cm radial extent and ~1 mm thickness

(b) Sections of a solid torus of ~ 5 mm thickness flanged at the access ports to provide the necessary toroidal electrical break.

The choice between the two solutions can only be made after a thorough design study and safety considerations regarding the tritium handling. The vacuum vessel, as the magnet, must provide access for the neutral injection.

If we assume the parameters for the neutral beam injection given in the appendix, namely a total power of 18 MW at an energy of 160 keV and a current density of 0·15 A/cm^2, we find a power density of 53 - 88 kW/cm^2. The present neutral injectors are available in units of 1 MW, then the required cross-section per 1 MW unit is 20·8 - 12·5 cm^2 and for a circular cross-section port the diameter would be 7·28 cm.

These numbers demonstrate that there is enough space in the device to allow the proposed neutral injection and also the design enables the possibility of more than one injector at each access port.

One technical difficulty could be the fraction of neutral beam passing through the plasma and depositing its energy on the opposite wall. From the operation of existing experiments this fraction could be about 5% and would mean a thermal wall loading opposite the injector of ~ 2.4 - 4.0 kW/cm^2. To lower the wall loading a corrugated surface could be used opposite to the injection ports combined with slightly non-perpendicular injection but this problem would require a detailed design study.

7. NUMERICAL RESULTS AND DISCUSSION

The differential equations (2.3)-(2.10) were solved numerically with a relative error tolerance of 10^{-7} and an absolute error tolerance of 10^{-4} using a variable order and variable step predictor-corrector method in double precision on a 32 bit word machine. The principal results are summarised in Figs. 1 - 10 and the table. The profile parameter δ was set equal to 1·4,

yielding $q_a = 2.53$; near radial injection was assumed and the conventional definition of β was used, with all fast particle effects included.

There are four main phases in the time evolution of the discharge and the four times marked A-D in Fig. 3 act as points of demarcation. The first phase corresponds essentially to the current rise when the plasma is ohmically heated to achieve the peak temperature $T_{i,o} = 2{\cdot}88$ keV and $T_{e,o} = 3{\cdot}10$ keV and the mean density is steadily increased to $\bar{n}_e = 2{\cdot}3 \times 10^{20}$ at the point A, $t = 420$ ms.

At the point A, when the temperature has reached ~ 3 keV the intense deuterium neutral beam injection is switched on and applied for 800 ms, until the point B, when $t = 1{\cdot}22$s. During this phase the cold neutral fuel gas supply is held steady at the value that was in force at A until $t = 1{\cdot}06$s and the increase in density during this phase shown in Fig. 3 is solely due to the effect of the beam. The intense deuteron beam has a significant effect on the tritium ratio ε, as illustrated in Fig. 8. To obtain a near optimum value of ε in the ignition phase it is necessary to start the discharge with a high concentration of tritium and carefully monitor the tritium ratio of the cold neutral gas surrounding the plasma.

The effect of the neutral beam heating on the peak plasma temperature is quite dramatic, at the point B $T_{i,o} = 17{\cdot}1$ keV and $T_{e,o} = 16.5$ keV. Fig. 9 shows that although initially the beam preferentially heats the electrons, i.e. $f_{Be} > 0{\cdot}5$, after the beam heating has been on for about 100 ms the situation is reversed and so, even though the alpha particle heating goes preferentially to the electrons, Figs. 5 and 6 show that the major energy source during the phase A-B is the beam heating of the ions. Consequently $T_i > T_e$, Fig. 3, and as a result of our assumption (5.6) about ion energy losses, the major losses are through the ion channel, as shown in Fig. 7. A noticeable feature of the phase A-B is the rapid decline in the ohmic heating power, Fig. 5, by about a factor of four as the plasma warms up. Fig. 5 illustrates very well the importance of the neutral injection heating in bridging the power gap when the ohmic power has declined considerably and the alpha particle heating has not built up to a sufficient level to take over as the dominant heating source.

Another interesting feature of the phase A-B is the large increase in β, from 0·304% to 3·40%, Fig. 8. During the intense neutral beam heating the device behaves essentially as a flux-conserving tokamak [15, 16]. The heating time

$\tau_H \simeq 3{\cdot}5\ \tau_E$, but τ_H is about an order of magnitude less than the magnetic diffusion time, τ_M, for the poloidal magnetic flux [17].

At the point B, when $t = 1{\cdot}06$s, cold neutral gas is puffed into the device to build up the plasma density in an effort to satisfy the ignition criterion on $\bar{n}\tau_E$. Several features are immediately apparent, (i) there is a drop in temperature as the main power source has to heat more plasma, Fig. 3, (ii) the fall in temperature causes an increase in ohmic power, Fig. 5, (iii) the increase in density causes an increase in bremsstrahlung losses, Fig. 7 and the net effect of the change in temperature and density is a decrease in the transport losses S^i_{tr} and S^e_{tr}, (iv) the reduced temperature and increased density cause a reduction in the slowing down times, Fig. 10, and this effect manifests itself particularly in peaks in the beam source functions in Figs. 5 and 6. The beam is switched off at $t = 1{\cdot}22$s. The increased plasma density causes a marked reduction in the beam coupling efficiency, Fig. 9.

The phase B-C is the one that determines whether full ignition is reached or not. The essence of the approach is that the cold gas supply to build up the density must not be too fast, or else the discharge could be quenched or disrupt, but the density build up must not be too slow either, otherwise the temperature can go below the ignition temperature before the $n\tau_E$ criterion is satisfied. The flux of cold gas used in the calculations shown in Fig. 3 is about the rate in the Alcator experiment [1,6]. The cold gas puffing is switched off at $t = 1{\cdot}24$s when $n\tau_E \simeq 4{\cdot}2 \times 10^{20}$ $m^{-3}s$. The average electron density is increased by a factor of 2 in 180 ms; in PLT $\bar{n}_e$ can be doubled in about 200 ms [22].

The final phase C-D represents the demonstration of ignition.

The calculation described above is only one of many that have been performed, and is close to the marginal case for ignition for our assumptions about transport losses. The conditions $\bar{T}_i = 6{\cdot}25$ keV and $n\tau_E = 4{\cdot}2 \times 10$ $m^{-3}s$ agree well with the calculations of Kesner and Conn [23]. The energy confinement time required, $\tau_E \simeq 550$ ms at ignition, is about five times less than the neo-classical value for ions in the banana regime under the same conditions and the density required, $\bar{n}_e \simeq 7{\cdot}5 \times 10^{20}$ has been obtained in Alcator [24] in a deuterium discharge with $B_T = 8{\cdot}7$ T.

Fielding and Haas [25, 26, 27] have investigated the mhd stability

of tokamaks with anisotropic pressure that would result from neutral injection heating and shown that it is the same as that for the equivalent scalar pressure tokamak for $\bar{p} = \frac{1}{2}(p_\perp + p_{||})$ constant on a flux surface, while near perpendicular injection can result in significant stabilization of high-n ballooning modes. However on the basis of ideal linear mhd scalar pressure stability theory [28] the value of β from our calculations, Fig. 8, would lead the plasma to be unstable to high-n ballooning modes. From recent calculations in which plasma equilibria have been first made stable to kink and tearing modes Wesson [29] quotes the critical β for high-n ballooning modes to be about 7 $(a/R_o)\%$, which in our case would give $\beta \simeq 2{\cdot}66\%$ which would invalidate our calculations and probably preclude the possibility of building an economic tokamak reactor. Fortunately there are several reasons for thinking that such a value of β might be unduly pessimistic : Robinson [30] claims to have reached a value of $\beta \simeq 2\%$ in the TOSCA tokamak whereas high n ballooning mode calculations for this device predict a critical β of $1{\cdot}3\%$ [25], but if the equilibrium is allowed to be unstable to high n modes a $\beta \simeq 2\%$ is obtained from the calculations. Even if the plasma equilibrium is unstable to high n ballooning modes the important point is the nonlinear saturation of the instability and the net effect might be a tolerable enhancement of transport losses.

If ballooning modes do not present a serious problem then the main limit on β is likely to arise from kink modes and idealized calculations indicate an upper limit of $0{\cdot}2$ (a/R_o) for the circular cross-section case [31] and $0{\cdot}37$ (a/R_o) for an elliptical cross-section with $b/a = 2{\cdot}2$ [32]. In our case these values would correspond to a β of $7{\cdot}6\%$ and $14{\cdot}0\%$ respectively. Hence it appears that an advantage might be gained in a non-circular cross-section device from the point of view of stability and also by increasing the energy confinement time by (b/a) [30].

8. CONCLUSIONS

We have described some transport calculations for a small ignition tokamak (SIT) which is based on the efficient use of ohmic heating [3], but with the recognition that additional heating, i.e. neutral injection, is necessary to achieve the ignition temperature, with puffing of cold neutral gas to attain the required plasma density. The conditions to be reached for ignition are $\bar{T}_i = 6{\cdot}25$ keV and $\bar{n}\tau_E = 4{\cdot}2 \times 10^{20} m^{-3} s$.

The calculations presented are of a preliminary nature and need to be supplemented by more complete computations in which additional physical effects, such as charge exchange losses [18], are included.

The engineering and technological aspects of the SIT rely upon proven technology and allow the possibility of optimisation at a later stage.

APPENDIX

Here we give the main physical and technological parameters.

Machine Parameters

R_o = 1·0 m

a = 0·38 m

B_T = 10 T

Plasma current I = 2·85 MA

Plasma current rise time = 350 ms

Plasma current plateau time ≃ 1·5 s

Toroidal Magnetic Parameters

Total coil current, I_M = 50 MA

current density, J_M = 113 A/mm^2

stresses, σ_M = 25.3 kg/mm^2

magnet radius, r_M = 0.42 m

stored energy ≃ 220 MJ

total energy to be supplied ≃ 500 MJ

dissipated power ≃ 100 MW

Ohmic transformer

one flux swing = 4.2 Wb

outer radius ≃ 0.40 m

Neutral injection

power = 18 MW

energy = 160 keV, D^o

current density ≃ 0.15 A/cm^2

number of units = 18 at 1 MW

Heating Cycle and Typical Plasma Parameters

Phase 1, O-A : ohmic heating phase lasting 0·42 s to give $T_{e,o}$ = 3·10 keV, $T_{i,o}$ = 2·88 keV with $\bar{n}_e = 2{\cdot}31 \times 10^{20}$

Phase 2, A-B : neutral injection phase. The neutral beam is switched on at 0·42 s and at a time of 1·06 s the peak temperatures are

$T_{e,o} = 16{\cdot}5$ and $T_{i,o} = 17{\cdot}1$ with $\bar{n}_e = 3{\cdot}65 \times 10^{20}$

Phase 3, B-C : end of neutral injection phase and puffing of cold neutral gas into the device to build up the plasma density. The neutral injection heating is continued until 1·22 s and cold gas is puffed into the device starting at 1·06 s until $\bar{n}_e \tau_e \simeq 4{\cdot}2 \times 10^{20}$ at 1·24 s , when $T_{e,o} = 11{\cdot}7$ keV, $T_{i,o} = 11{\cdot}4$ keV with $\bar{n}_e = 7{\cdot}47 \times 10^{20}$.

Phase 4, C-D : controlled thermonuclear fusion and self-sustaining nuclear heating balancing all power losses. $T_{e,o} = 11{\cdot}9$ keV, $T_{i,o} = 11{\cdot}5$, $\bar{n}_e = 7{\cdot}41$.

REFERENCES

[1] APGAR, E., et al, in "Plasma Physics and Controlled Fusion Research", Vol.1, (1977), 247, IAEA, Vienna.

[2] TERRY, J.L., et al, Nucl. Fusion 18 (1978), 485.

[3] COPPI, B., Comments on Plasma Phys. Cont. Fusion 3 (1977), 47.

[4] FIELD, J.J. and MINARDI, E., "Transport calculations for a high density ohmically heated D-T Tokamak". CLM-R 191.

[5] JASSBY, D.L., TOWNER, H.H. and GOLDSTON, R.J. Nucl. Fusion 18 (1978), 825.

[6] HUGHES, M.H., Princeton Report PPPL 1411 (1978).

[7] COHN, D.R., PARKER, R.R. and JASSBY, D.L. Nucl. Fusion 16 (1976), 31.

[8] SWEETMAN, D.R., Nucl. Fusion 13 (1973), 157.

[9] BUTLER, S.T. and BUCKINGHAM, M.J., Phys. Rev. 126 (1962), 1.

[10] MILEY, G.H., TOWNER, H. and IVICH, N. University of Illinois, Urbana Report COO-2218-17 (1974).

[11] BRUNELLI, B., CNEN Report 78/11P. This expression is a fit to the results of MILEY et al. [10].

[12] ROSENBLUTH, M.N., Nucl. Fusion 10 (1970), 340.

[13] ENGELMANN, F. and CURATOLO, M., Comments on Plasma Phys. Cont. Fusion 1 (1972), 121.

[14] KRALL, N.A. and McBRIDE, J.B., Nucl. Fusion 17 (1977) 713.

[15] CLARKE, J.F., ORNL/TM 5429 (1976).

[16] DORY, R.A. and PENG, Y.-K.M., Nucl Fusion 17 (1977) 21.

[17] CALLEN, J.D., Comments on Plasma Phys. Cont. Fusion 2 (1976), 159.

[18] EUBANK, H., et al., IAEA-CN-37-C-3, Innsbruck (1978).

[19] The tokamak design group - the Frascati tokamak, Proc. 7th SOFT Conference (1972), 207.

[20] ANZIDEI, L., et al., Proc. 8th SOFT Conference (1974), 209.

[21] ANDREANI, R., et al., Proc. 8th SOFT Conference (1974), 177.

[22] GROVE, D., et al. in "Plasma Physics and Controlled Fusion Research", Vol. I (1977), 21, IAEA, Vienna.

[23] KESNER, J. and CONN, R.W., Nucl. Fusion 16 (1976), 397.

[24] GONDHALEKAR, A., et al., IAEA-CN-37-C-4, Innsbruck (1978).

[25] SYKES, A., TURNER, M.F., FIELDING, P.J. and HAAS, F.A., IAEA-CN-37-K-5, Innsbruck (1978).

REFERENCES (continued)

[26] FIELDING, P.J. and HAAS, F.A.,Phys. Rev. Lett. 41 (1978), 801.

[27] FIELDING, P.J. and HAAS, F.A., to be published.

[28] CONNOR, J.W., HASTIE, R.J. and TAYLOR, J.B., Phys. Rev. Lett. 40 (1978), 396.

[29] WESSON, J.A., (private communication).

[30] McGUIRE, K., ROBINSON, D.C. and WOOTTON, A.J., IAEA-CN-37-T-1-1, Innsbruck (1978).

[31] FREIDBERG, J.P. and HAAS, F.A., Phys. Fluids 16 (1973), 1909.

[32] FREIDBERG, J.P. and HAAS, F.A., Phys. Fluids 17 (1974), 440.

[33] WAGNER, C.E. and STUART, G.W., SIA Report No. LAPS-35 SAI-77-982-LJ.

MAIN PLASMA PARAMETERS AT VARIOUS TIMES DURING THE DURATION OF THE DISCHARGE

Point in Fig. 3	A	B	C	D
time , s	0·42	1·06	1·24	1·76
$n_{e,o}$, 10^{20} m^{-3}	3·92	6·2	12·7	12·6
$\bar{n}_e$, 10^{20} m^{-3}	2·31	3·65	7·47	7·41
$\bar{n}_\alpha$, 10^{20} m^{-3}	$7·4 \times 10^{-6}$	$1·3 \times 10^{-2}$	$2·25 \times 10^{-2}$	$5·09 \times 10^{-2}$
$T_{i,o}$, keV	2·88	17·1	11·4	11·5
$T_{e,o}$, keV	3·10	16·5	11·7	11·9
$\bar{T}_i$, keV	1·58	9·38	6·25	6·31
τ_{Ee} , ms	169	268	548	545
$\bar{n}\tau_E$, 10^{20} m^{-3} s	0·42	0·935	4·2	4·11
β , %	0·304	3·40	4·36	4·34
β_p	0·135	1·51	1·94	1·93
S^e_Ω , MW m^{-3}	1·18	$1·41 \times 10^{-1}$	$2·1 \times 10^{-1}$	$2·07 \times 10^{-1}$
S^e_B , MW m^{-3}	$3·3 \times 10^{-1}$	1·49	$4·01 \times 10^{-1}$	–
S^e_α , MW m^{-3}	$2·11 \times 10^{-3}$	1·93	4·70	4·24
$S^e_{B\alpha}$, MW m^{-3}	$6·71 \times 10^{-3}$	$3·20 \times 10^{-1}$	$5·52 \times 10^{-2}$	–
S^e_{br} , MW m^{-3}	$-4·18 \times 10^{-2}$	$-2·43 \times 10^{-1}$	$-8·57 \times 10^{-1}$	$-8·6 \times 10^{-1}$
S^e_{cy} , MW m^{-3}	$-4·41 \times 10^{-3}$	$-1·57 \times 10^{-1}$	$-1·14 \times 10^{-1}$	$-1·16 \times 10^{-1}$
S^e_{tr} , MW m^{-3}	$-5·55 \times 10^{-1}$	$-2·95$	$-2·10$	$-2·13$
S^i_α , MW m^{-3}	$7·06 \times 10^{-5}$	$3·51 \times 10^{-1}$	$6·11 \times 10^{-1}$	$5·59 \times 10^{-1}$
S^i_B , MW m^{-3}	$1·2 \times 10^{-1}$	3·99	$6·98 \times 10^{-1}$	–
$S^i_{B\alpha}$, MW m^{-3}	$2·24 \times 10^{-4}$	$5·84 \times 10^{-2}$	$7·18 \times 10^{-3}$	–
S^i_{tr} , MW m^{-3}	$-4·79 \times 10^{-1}$	$-3·17$	$-1·97$	$-1·99$
S^i_Δ , MW m^{-3}	$5·38 \times 10^{-1}$	$-3·73 \times 10^{-1}$	1·39	1·38
$f_{\alpha e}$	0·968	0·846	0·885	0·884
f_{Be}	0·733	0·272	0·365	0·361
τ_α , ms	24·7	105	36·1	36·9
τ_B , ms	21·7	42·1	18·0	18·2
P_α	0·703	0·703	0·703	0·703
P_B	0·899	0·899	0·899	0·899
C_{eff}	1·00	0·89	–	–
ε	0·710	0·495	0·490	0·493

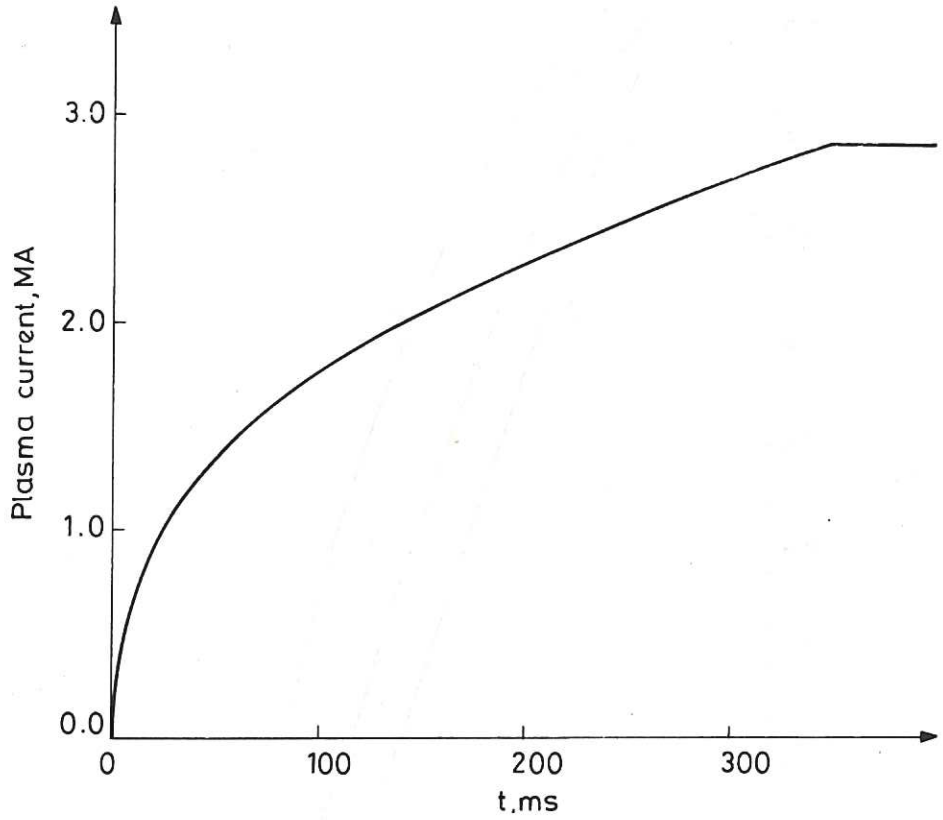

Fig.1 Profile for current rise in plasma.

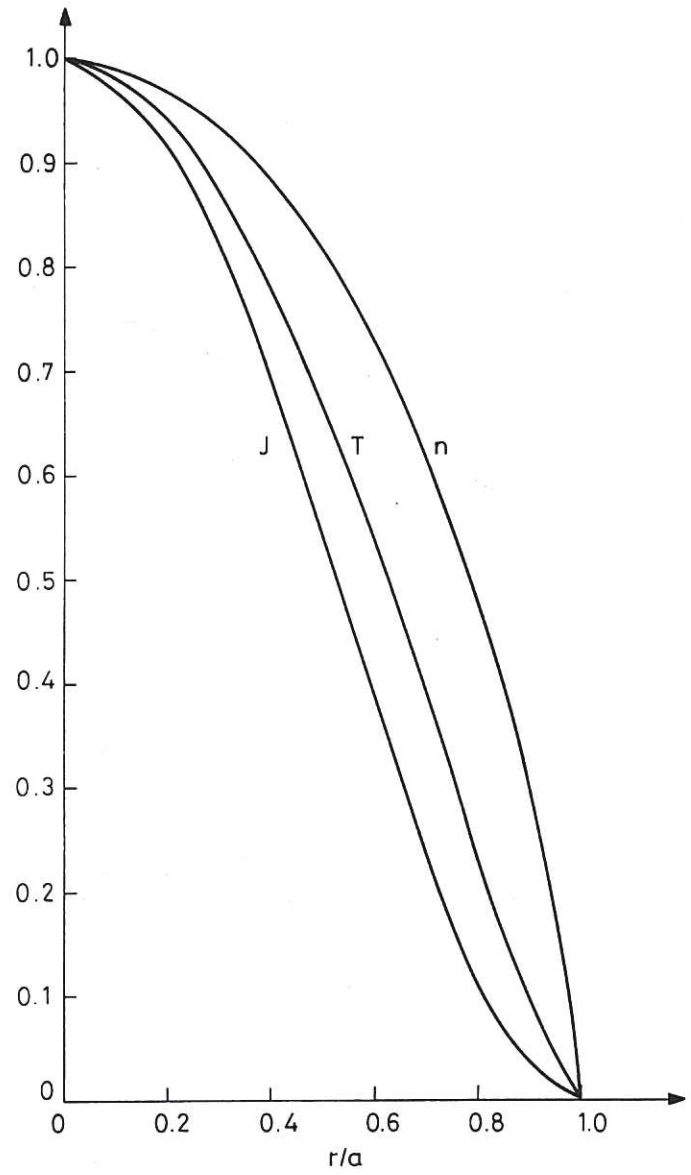

Fig.2 Profiles for n and T used in averaging over the radial coordinate in the transport equation. The current density profile is calculated on the basis of Spitzer resistivity and is used to estimate q.

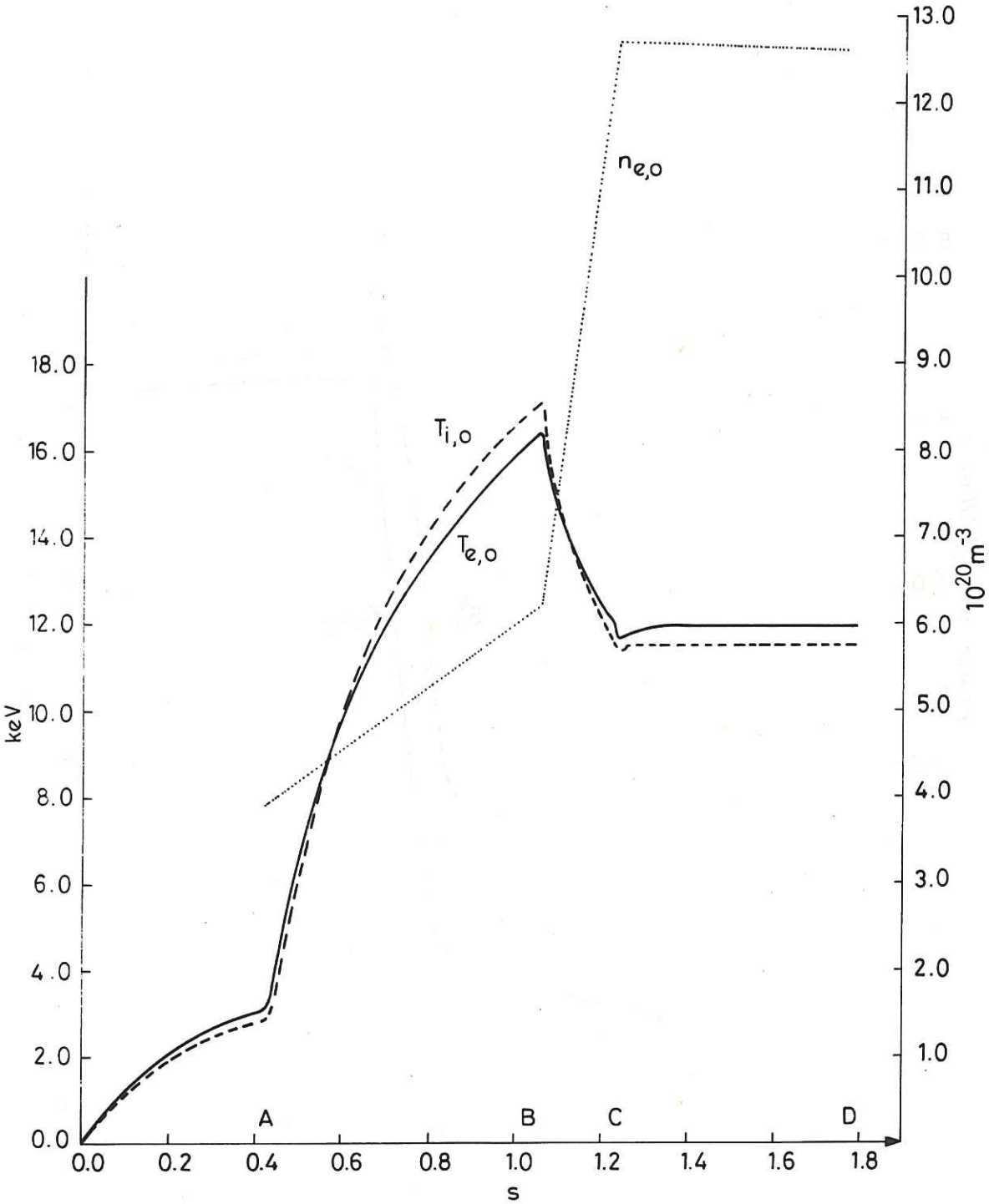

Fig.3 Time evolution of the electron and ion temperatures and electron density on axis.

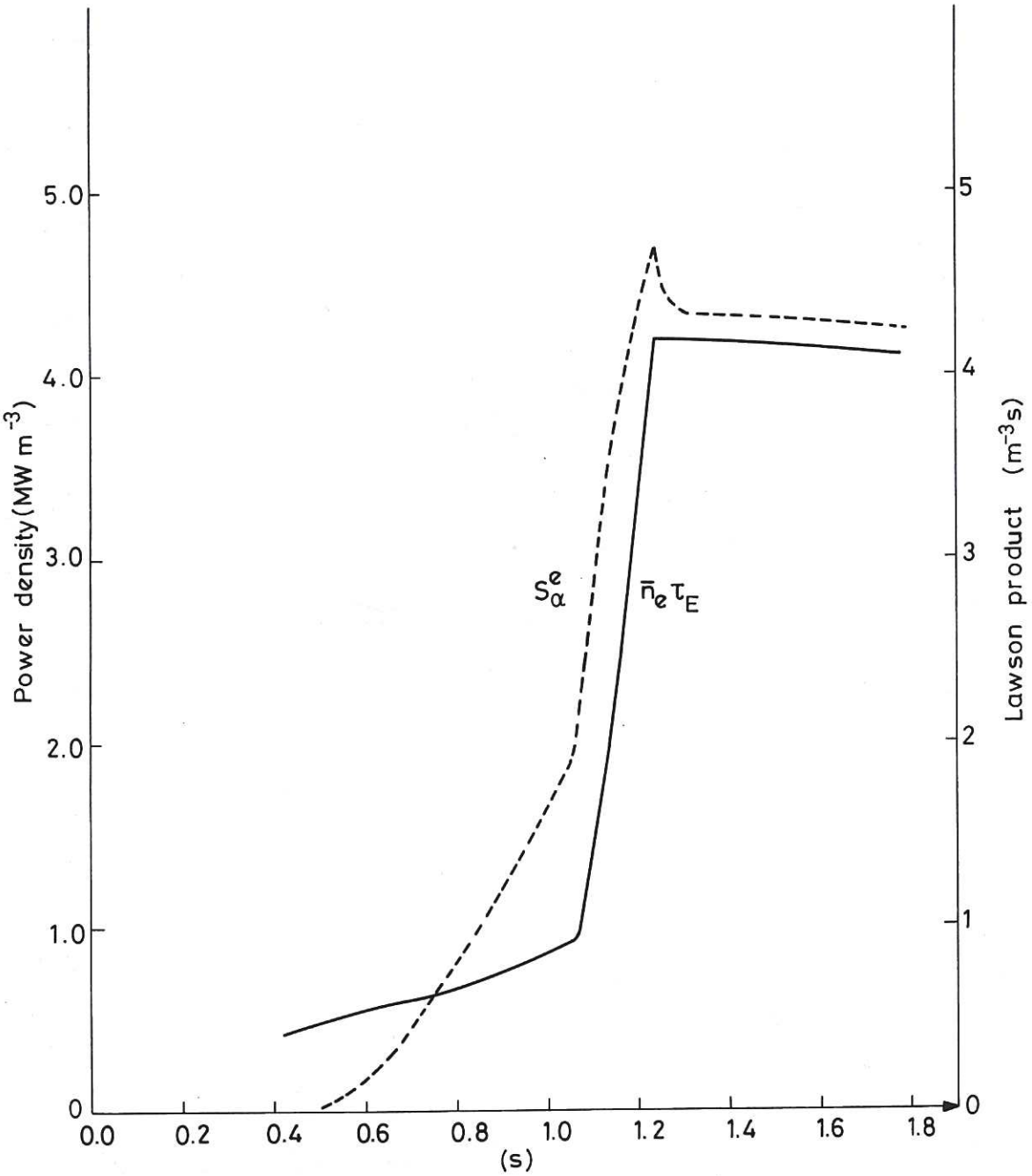

Fig.4 Time evolution of the source of alpha heating to the electrons and of the Lawson product.

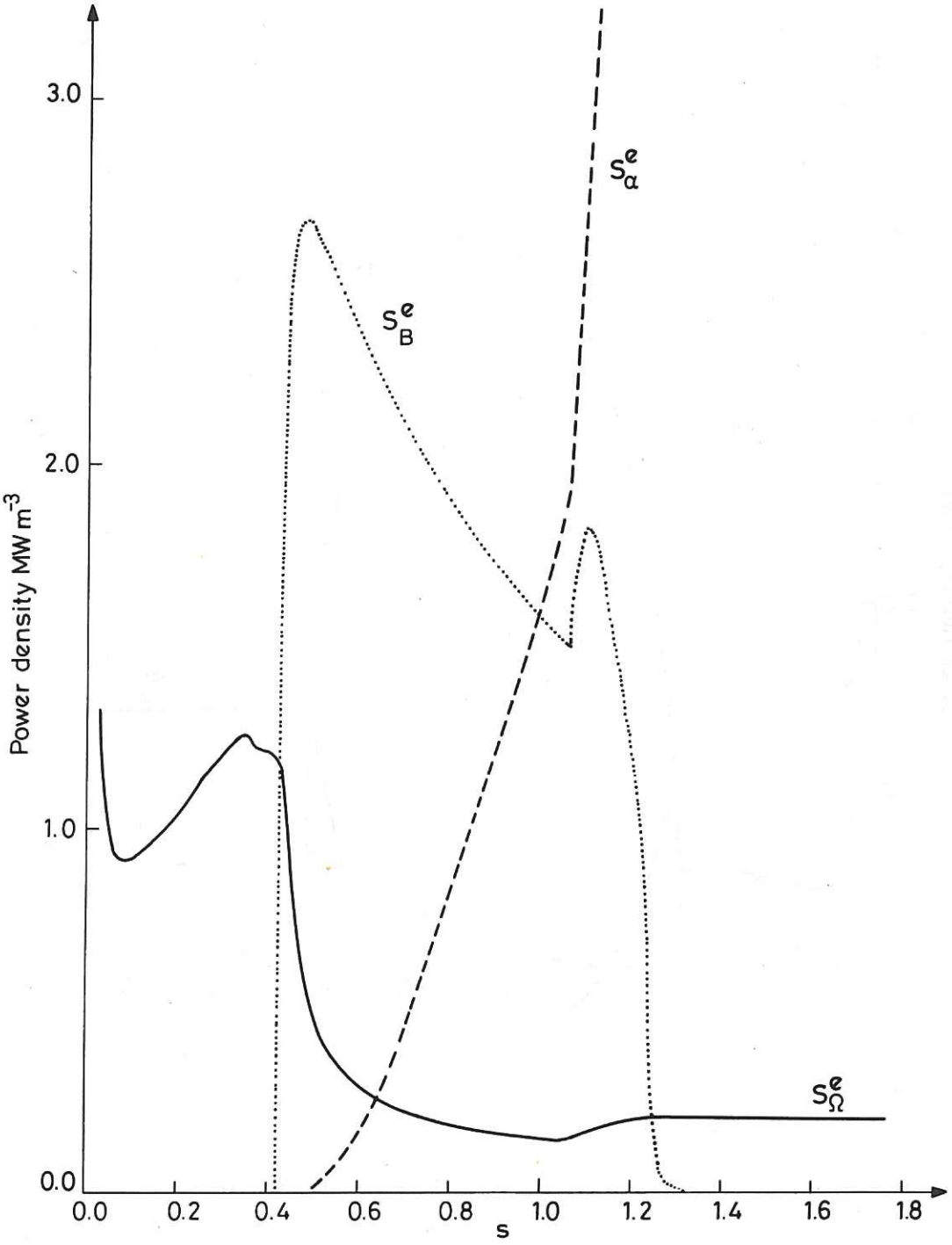

Fig.5 Time evolution of the main electron energy sources.

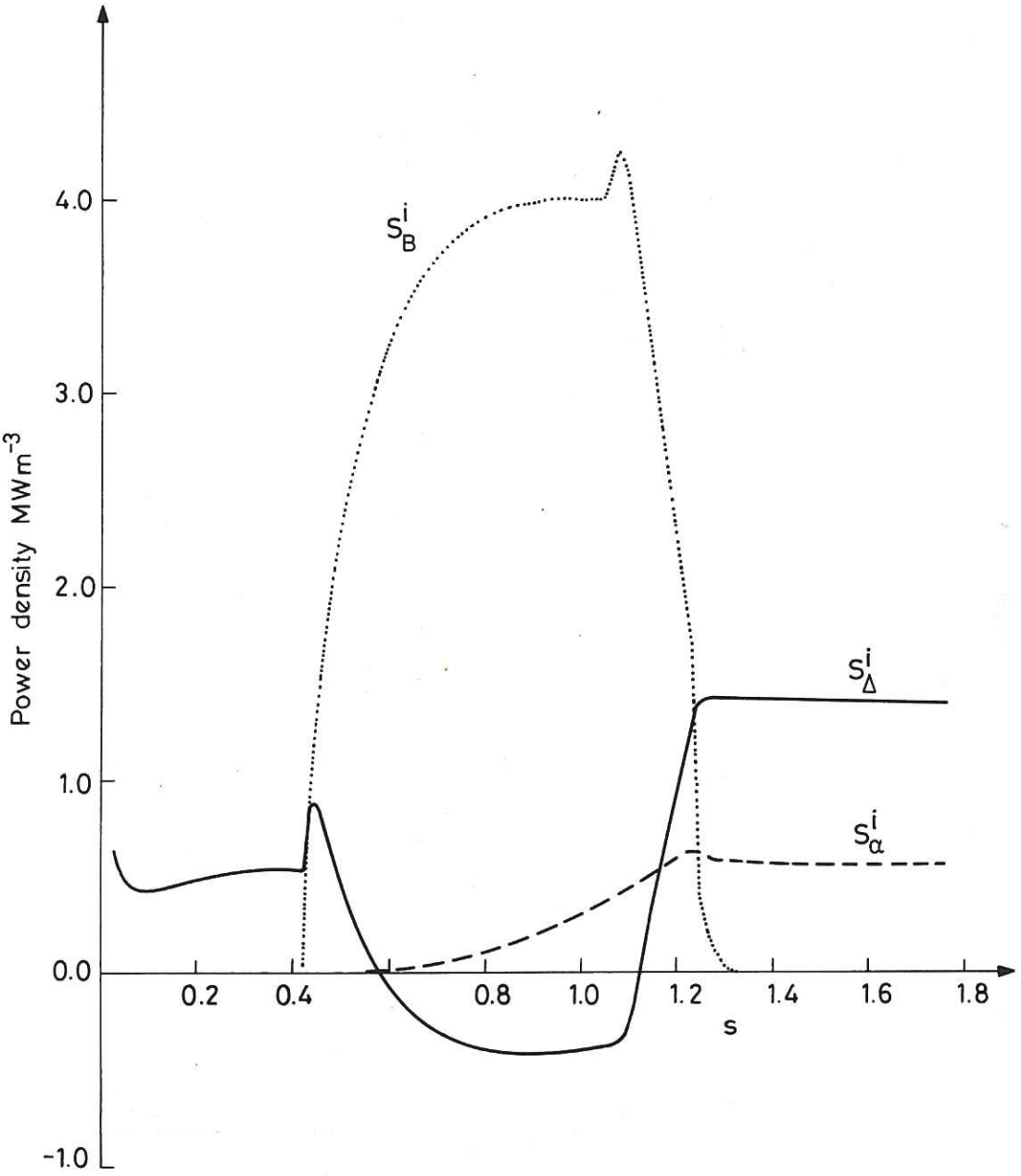

Fig.6 Time evolution of the main ion energy sources.

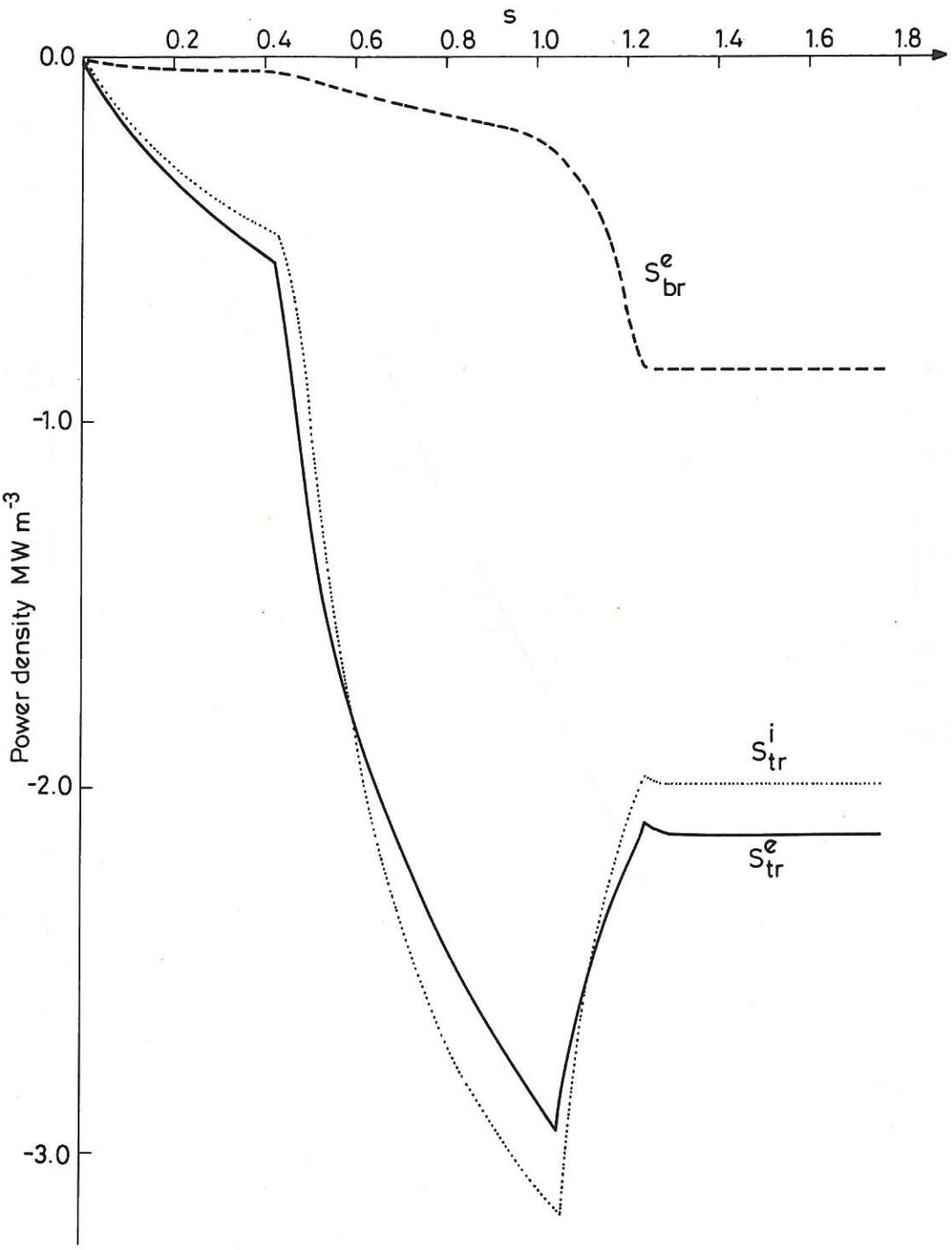

Fig.7 Time evolution of the main energy sinks.

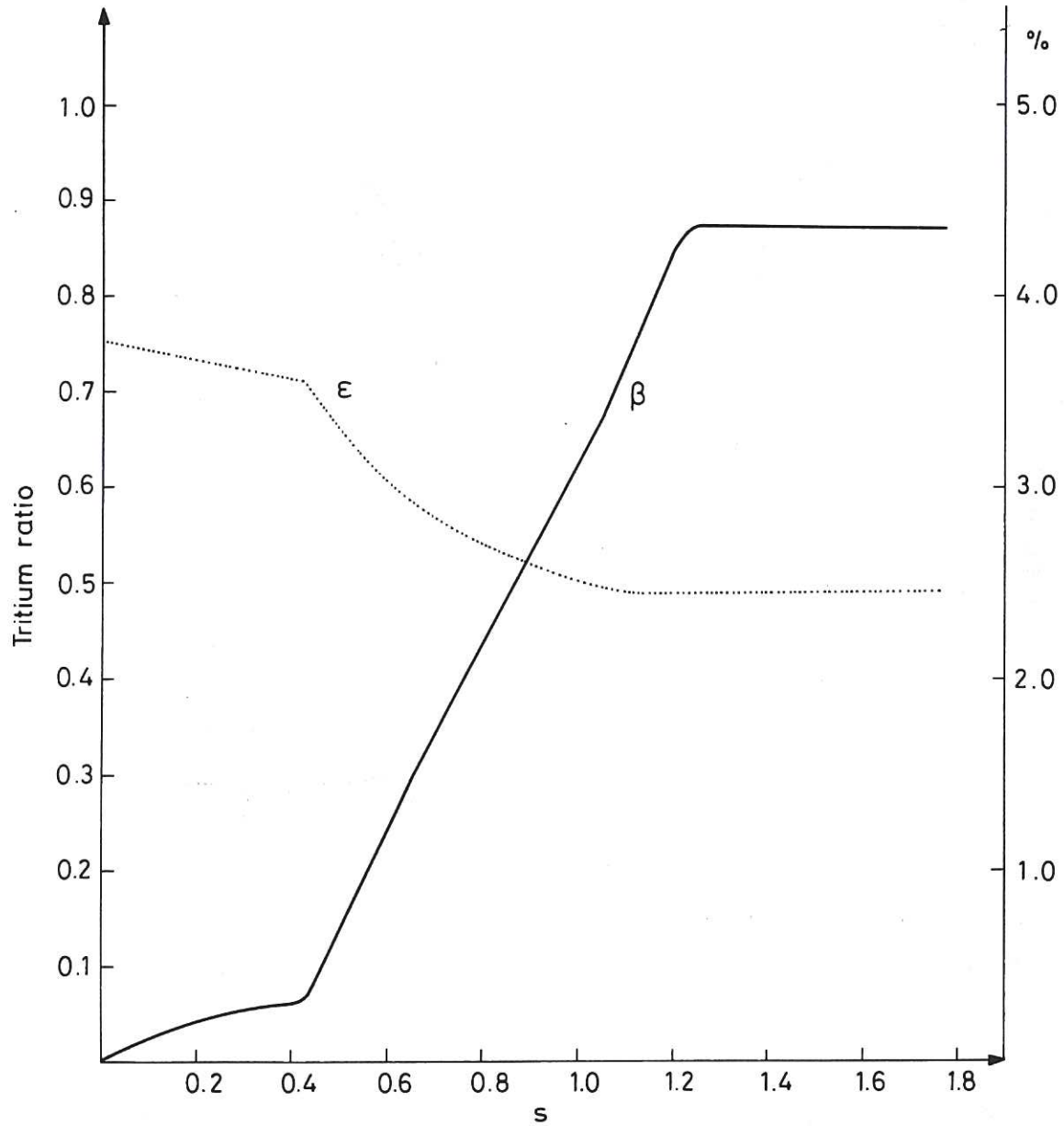

Fig.8 Time variation of the tritium ratio ϵ and the total β, including all fast particle contributions.

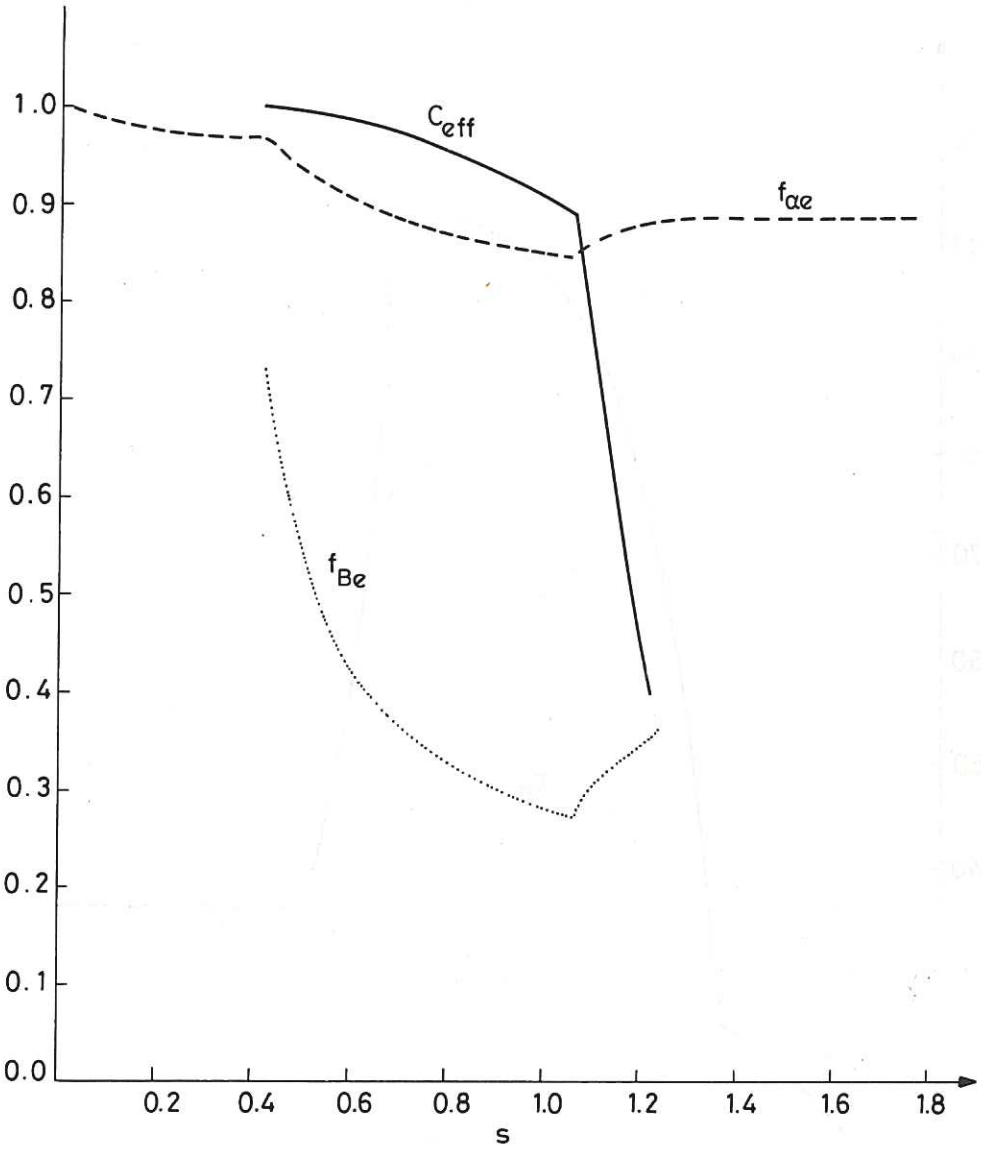

Fig.9 Time variation of the fraction of alpha particle energy going to the electrons, $f_{\alpha e}$, the fraction of beam energy going to the electrons, f_{Be}, and the beam coupling efficiency, C_{eff}.

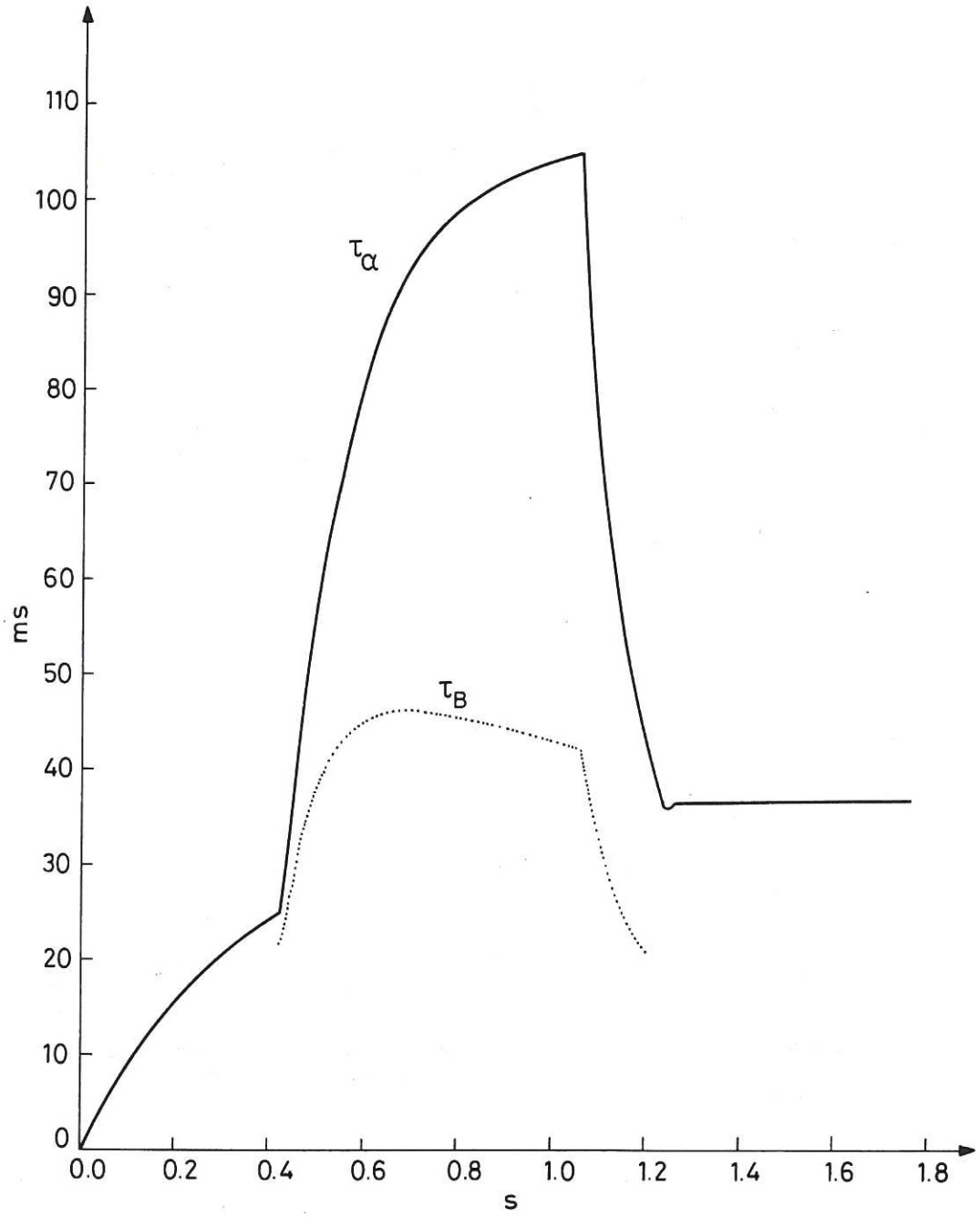

Fig.10 Time variation of the alpha particle slowing down time, τ_α and the beam slowing down time τ_B.

HER MAJESTY'S STATIONERY OFFICE

Government Bookshops

49 High Holborn, London WC1V 6HB
13a Castle Street, Edinburgh EH2 3AR
41 The Hayes, Cardiff CF1 1JW
Brazennose Street, Manchester M60 8AS
Wine Street, Bristol BS1 2BQ
258 Broad Street, Birmingham B1 2HE
80 Chichester Street, Belfast BT1 4JY

Government publications are also available through booksellers